Biological Psychiatry: CNNI

Archival Report

Altered Brain Network Dynamics in Schizophrenia: A Cognitive Electroencephalography Study

Jodie Naim-Feil, Mica Rubinson, Dominik Freche, Alexander Grinshpoon, Abraham Peled, Elisha Moses, and Nava Levit-Binnun

ABSTRACT

BACKGROUND: Alterations in the dynamic coordination of widespread brain networks are proposed to underlie cognitive symptoms of schizophrenia. However, there is limited understanding of the temporal evolution of these networks and how they relate to cognitive impairment. The current study was designed to explore dynamic patterns of network connectivity underlying cognitive features of schizophrenia.

METHODS: In total, 21 inpatients with schizophrenia and 28 healthy control participants completed a cognitive task while electroencephalography data were simultaneously acquired. For each participant, Pearson cross-correlation was applied to electroencephalography data to construct correlation matrices that represent the static network (averaged over 1200 ms) and dynamic network (1200 ms divided into four windows of 300 ms) in response to cognitive stimuli. Global and regional network measures were extracted for comparison between groups.

RESULTS: Dynamic network analysis identified increased global efficiency; decreased clustering (globally and locally); reduced strength (weighted connectivity) around the frontal, parietal, and sensory-motor areas; and increased strength around the occipital lobes (a peripheral hub) in patients with schizophrenia. Regional network measures also correlated with clinical features of schizophrenia. Network differences were prominent 900 ms following the cognitive stimuli before returning to levels comparable to those of healthy control participants.

CONCLUSIONS: Patients with schizophrenia exhibited altered dynamic patterns of network connectivity across both global and regional measures. These network differences were time sensitive and may reflect abnormalities in the flexibility of the network that underlies aspects of cognitive function. Further research into network dynamics is critical to better understanding cognitive features of schizophrenia and identification of network biomarkers to improve diagnosis and treatment models.

Keywords: Cognition, Connectivity, Dynamics, Graph theory, Network, Schizophrenia

http://dx.doi.org/10.1016/j.bpsc.2017.03.017

Schizophrenia (SCH) is a complex and devastating psychiatric disorder whose underlying neurobiological mechanisms are still unknown. Cognitive dysfunction is a multifaceted and complex feature of SCH and is commonly associated with poor treatment outcomes (1). Many of these cognitive processes rely on brain circuitry such as the frontal and parietal regions (2), the same regions altered in SCH (3,4). Therefore, there appears to be an intricate relationship between cognitive impairment and the pathophysiology of SCH. The current study was designed to examine altered network connectivity patterns underlying various cognitive features of SCH and to explore the dynamic nature of these network anomalies.

Recently, topological measures that apply network analysis based on graph theory to neuroimaging data have been used to characterize global network properties of the brain (5–7). This approach is particularly pertinent to the study of SCH, which is described as the prototypical disease of brain dysconnectivity (8,9). Indeed, a growing number of studies have revealed network abnormalities in patients with SCH such as altered network measures of connectivity, efficiency, and integration (10). While these network findings are largely based on a static network representation of the SCH brain, there is a growing interest in the dynamic changes of network connectivity (11–13). Static network representations are derived from a network constructed by encapsulating neuroimaging data from an entire scan session (resting state or task activated). However, higher-order brain functions, such as executive function, require dynamic brain coordination that can occur on the order of milliseconds (14). To examine the dynamic connectivity changes that underlie specific features of cognition, recent studies in healthy control (HC) participants have applied network analysis to shorter time intervals and constructed functional networks for each of these time intervals to quantify how these networks change over time (15,16). Using this approach, recent functional magnetic resonance imaging studies have demonstrated dynamic reconfiguration of network connectivity patterns following administration of

 ISSN: 2451-9022

cognitive stimuli (13,17,18), while transient changes (on the order of seconds and milliseconds) in network states have been detected by magnetoencephalography (19) and electroencephalography (EEG) (14,20,21). Although network analysis traditionally has been performed on functional magnetic resonance imaging data, these EEG and magnetoencephalography studies highlight the temporal benefits of using physiological techniques to explore the rapid reconfiguration of functional brain networks underlying various aspects of cognition (20).

Given that impaired cognition is a key feature of SCH (1), the quantification of altered patterns of network connectivity underlying these deficits will help to identify aberrant global network properties of SCH (22–24). Preliminary EEG network (static) studies have demonstrated various network connectivity alterations across working memory (25–28) and auditory oddball (29) tasks in patients with SCH. The current study was designed to expand on these static network studies by applying dynamic network methodology and using the temporal advantages of EEG to explore the functional dynamic network organization underlying specific cognitive impairments associated with SCH.

To achieve this, we administered a robust and sensitive cognitive task called the Sustained Attention to Response Task (SART) (30). The SART provides a measure of response inhibition and sustained attention (31) and has been applied to identify clinically relevant cognitive impairments in patients with SCH (32–34). Successful performance on the SART requires activation of a number of widespread and spatially distributed brain regions in selecting and integrating those cognitive stimuli that are considered task relevant while suppressing irrelevant stimuli (35,36). In the current study, cognitive stimuli from the SART were used as a perturbation tool to elicit a transient change within the network organization while EEG measured the functional dynamics of the network response to the cognitive stimuli, thereby enabling us to quantify how these connectivity patterns differ in patients with SCH.

The current study had two major objectives: 1) characterize global properties of network connectivity (elicited by cognitive stimuli from the SART) underlying specific cognitive impairment in patients with SCH compared with HC participants and 2) apply dynamic network analysis to explore whether these patterns of network connectivity evolve over time and differ in patients with SCH.

METHODS AND MATERIALS

The current study was approved by the Shaar Menashe Mental Health Center institutional ethics review committee. Participants received the equivalent of $25 (U.S.) reimbursement for participation.

Subjects

A total of 25 in-unit patients with SCH at Shaar Menashe Mental Health Center meeting the criteria for DSM-IV-TR schizophrenia (37) were recruited. Patients with SCH with a history of neurology disorders, comorbidity, and drug abuse were excluded from the study. Of the sample, 2 SCH datasets were excluded due to the participants' inability to understand the task requirements, and another 2 datasets were excluded due to excessive head movement. As such, 21 SCH datasets were analyzed. A trained psychiatrist administered the Scale for the Assessment of Positive Symptoms (38) and the Scale for the Assessment of Negative Symptoms (39) to assess clinical symptoms of SCH and administered the Neurological Evaluation Scale (40) to index soft neurological signs.

A total of 30 HC participants without any previous or current history of psychiatric illness, or alcohol/drug dependence or abuse or head injury, were recruited through local advertisements. Of the sample, 2 HC datasets were excluded due to preexisting psychiatric conditions. As such, 28 HC datasets were analyzed.

All participants completed a general demographic questionnaire (Table 1).

Experimental Design

Participants had the BioSemi head-cap (BioSemi, Amsterdam, The Netherlands) consisting of 64 EEG sensors (10/20 international system) placed on their head. EEG signals were recorded by the BioSemi ActiveTwo EEG measurement system using Ag-AgCl active electrodes. EEG signals were digitized online at a sampling rate of 1024 Hz. Once the EEG was set up, participants completed the computerized SART (see the Supplement) (30) using E-Prime version 2 technology (Psychology Software Tools, Pittsburgh, PA), which sent triggers to the BioSemi system via a USB relay (KMTronic USB

Table 1. Demographic, Clinical, and Behavioral Data (Performance on the SART) for Patients With Schizophrenia and Healthy Control Participants

	Patients With Schizophrenia[a] (n = 21)	Healthy Control Participants (n = 28)	p Value
Age, Years	38 ± 12	34 ± 10	.244
Gender (Male:Female)	14:7	18:10	.862
Education, Years	13 ± 1	15 ± 1	.001[b]
Handedness (Right:Left)	20:1	27:1	.835
Duration of Illness, Years	12 ± 7	NA	NA
Hospitalizations	9 ± 9	NA	NA
SAPS Total	35 ± 16	NA	NA
SANS Total	82 ± 18	NA	NA
SANS Attention Subscale	8 ± 2	NA	NA
NES Total	2 ± 1	NA	NA
SART RT	475 ± 74	379 ± 44	< .001[b]
SART Intravariability	0.26 ± 0.07	0.18 ± 0.05	< .001[b]
SART Omission Errors	16 ± 18	0 ± 2	.001[b]
SART Commission Errors	9 ± 8	6 ± 4	< .001[b]

Data are mean ± SD or n.

NA, not applicable; NES, Neurological Evaluation Scale; RT, reaction time; SANS, Scale for the Assessment of Negative Symptoms; SAPS, Scale for the Assessment of Positive Symptoms; SART, Sustained Attention to Response Task.

[a]Medication: in patients with schizophrenia, 38% received atypical antipsychotics (olanzapine or risperidone) and 62% received typical antipsychotics (zuclopenthixol depot injections, haloperidol, perphenazine, or levomepromazine).

[b]$p < .01$.

Relay; KMTronic, Veliko Turnovo, Bulgaria) to provide a time-stamp of the stimuli presentation in the EEG recording.

EEG Processing

EEG recordings were processed offline using the EEGLAB open source toolbox (41), in-house MATLAB scripts (The MathWorks, Inc., Natick, MA), and the Brain Connectivity Toolbox (42). EEG preprocessing stages are described in the Supplement. For the static network analysis, epoch duration was 0 to 1200 ms following stimuli presentation and averaged over trials. For the dynamic network analysis, each epoch was divided into five equal-length time windows of 300-ms duration following stimuli presentation and averaged over trials: window 1 (−350 to −50 ms), window 2 (0 to 300 ms), window 3 (300 to 600 ms), window 4 (600 to 900 ms), and window 5 (900 to 1200 ms) (illustrated in Supplemental Figure S1).

Network Construction

EEG data traces are used to generate connectivity graphs that provide a simplified representation of brain network activity during a fixed time span. We define such a time span, which consists of discrete time points, as all sample points of the gradient montage signals $V_i[t]$ (i =1, …, 139) with t between 0 and a given duration T. The gradient montage is similar to the bipolar, sequential, and Laplacian montages yet gives more local information while reducing artifacts induced by global long-range correlations. The reference choice is detailed in the Supplement. The graph (also called network) that we construct consists of a set of vertices (or nodes) V and a set of edge weights (or connections) E between any two vertices in the graph. The nodes represent signals for the defined time span, which we therefore also denote by V_i. To define the edge e_{ij} between two nodes V_i and node V_j, we compute the normalized pairwise Pearson cross-correlation coefficient over the given time span for a given time delay τ,

$$c(\tau) = \left(\frac{1}{T-1}\right) \frac{\sum_t \left[\left(V_i[t]-\overline{V}_i\right)\cdot\left(V_j[t-\tau]-\overline{V}_j\right)\right]}{\sqrt{\sum_t \left(V_i[t]-\overline{V}_i\right)^2}\cdot\sqrt{\sum_t \left(V_j[t-\tau]-\overline{V}_j\right)^2}}$$

where $\overline{V}_i$ is the time average of V_i. The delay τ was chosen to range between 0 and 150 ms to account for cross-cortical conduction times and for known neurophysiological processes (43). Considering the maximal delay τ (up to 150 ms) allowed us to construct a directed network. An edge e_{ij} is then defined as the maximum of $c(\tau)$ over all τ. If $e_{ij} > e_{ji}$, we keep only e_{ij} and set e_{ji} to zero. The e_{ij} defined in this way reflects a statistical dependence of the signals between the nodes during the fixed time span. The resulting graph is both directed (i.e., all edges are directed from one vertex to another) and weighted (the edges retain their correlation coefficient index). Individual networks were constructed for the static network and for each of the five time windows comprising the dynamic network of each participant. For each of these networks, a proportional threshold was applied to remove weak or artifactual statistical correlations (i.e., edge weights close to 0) (see the Supplement). In the Results section, we present the network data extracted when the proportional density threshold is set at 30% for all graphs (mean degree = 76) (22).

Network Analysis

Degree (k). The degree k of a node refers to the number of edges connecting to or from the node. Nodes with a high degree have increased connectivity with the other vertices and can be considered as representing hubs in the network (see the Supplement). In a directed network, the degree is the sum of inward links (in-degree) and outward links (out-degree).

Strength (Measure of Node Influence). The strength (or weight) of a node is defined as the sum of all edge weights (i.e., strength of the links) connected to the node. The directed in-strength and out-strength of node V_i are defined as $k_i^{win} = \sum_{j\in N} e_{ji}$ and $k_i^{wout} = \sum_{j\in N} e_{ij}$, respectively.

Clustering Coefficient (Measure of Segregation). The clustering coefficient (CC) C_i quantifies how likely it is for two neighbors of the same node V_i to be connected, producing a triangle in the graph. C_i provides information about the local connectivity and structure within a network (44). If t_i is the number of triangles that node V_i participates in, then $C_i = 2t_i/k_i(k_i-1)$, where k_i is the degree of node V_i. The global CC of a graph is calculated as the average CC of all nodes.

Path Length and Global Efficiency (Measure of Integration). The path length L_{ij} is defined as the minimum number of edges needed to pass from node V_i to node V_j. We set $L_{ij} = \infty$ for any disconnected node pairs V_i and V_j. The global efficiency GE is defined as the average inverse path length distance in the network $GE = \frac{1}{|V|(|V|-1)}\sum_{i,j,j\neq i} L_{ij}^{-1}$ where $|V|$ denotes the number of vertices in V. GE measures the overall capacity for integrated processing of the network.

Statistical Analysis

Comparability of patients with SCH and HC participants basic demographics were assessed using chi-square tests for categorical variables and t tests for continuous variables (Table 1). Given the need for rigorous appraisal of our novel approach and to address cases of violations of unequal variance, we applied a conservative alpha level of $p < .01$ for all statistical tests. All data analyses were performed using SPSS for Windows, version 15 (SPSS Inc., Chicago, IL). For all behavioral and network metrics, analysis of variance was applied to measure group differences. After careful inspection of the scatterplots, we used the nonparametric Spearman rank-order correlation to avoid excessive influence of outliers when examining the relationship between these variables. The receiver operating characteristic (ROC) curve analysis was implemented to examine the ability for the network metrics to discriminate between patients with SCH and HC participants (see Supplement).

RESULTS

Behavioral Results

As expected, the SCH group made significantly more errors of omission (GO: not pressing when required to press) and commission (NOGO: pressing when required to withhold) than

the HC group ($F_{1,20.39}$ = 215.05, p = .001, and $F_{1,46}$ = 36.43, $p \leq .005$, respectively). Patients with SCH presented with increased reaction time ($F_{1,47}$ = 32.13, $p \leq .005$, and performance variability, $F_{1,47}$ = 21.46, $p \leq .005$), compared with HC participants (Table 1).

Network Results

Global Measures: Clustering Coefficient. At baseline, there were no significant differences between groups (Table 2). For the static network (0–1200 ms), the SCH group exhibited significantly reduced CC relative to the HC group in both the GO and NOGO conditions. In the dynamic network, the SCH group presented with reduced CC in windows 2, 3, and 4 during the GO condition and in windows 2 and 3 during the NOGO condition. By window 5, there were no significant differences between the groups (Figure 1).

Global Measures: Global Efficiency. At baseline, we observed no significant differences between groups. For the static network (0–1200 ms), there were no significant differences in global efficiency (GE) between groups across the GO and NOGO conditions. In contrast, the dynamic network analysis uncovered a clear difference in network response between the groups, with the SCH group presenting with significantly increased GE at windows 2 and 3 for both the GO and NOGO conditions. By windows 4 and 5, there were no significant differences between the groups (Figure 1).

Regional Measures: Clustering Coefficient. In the GO condition, at baseline the SCH group presented with a reduced CC in the frontal regions. For the static network, patients with SCH had a reduced CC around the frontal and parietal regions. In the dynamic network, patients with SCH presented with reduced CC around the frontal, temporal, sensory-motor, and parietal regions at window 2 and with reduced CC in the frontal and sensory-motor regions at window 3. No significant differences between groups were observed at windows 4 and 5.

In the NOGO condition, at baseline there were no significant differences between groups. In the static network, the SCH group demonstrated reduced CC around the frontal, temporal, sensory-motor, parietal, and occipital regions. In the dynamic network, patients with SCH showed reduced CC around the

Table 2. Global Connectivity Measures: Global Efficiency and Clustering Coefficient Network Metrics Across the GO and NOGO Conditions in Patients With Schizophrenia and Healthy Control Participants

	Patients With Schizophrenia (n = 21)	Healthy Control Participants (n = 28)	F Value, df = (1,47)	p Value
Global Efficiency GO				
Baseline	0.47 ± 0.06	0.47 ± 0.04	0.001	.976
Static window (0–1200 ms)	0.44 ± 0.04	0.43 ± 0.06	0.26	.613
Window 2 (0–300 ms)	0.40 ± 0.06	0.34 ± 0.04	16.02	< .001[a]
Window 3 (300–600 ms)	0.39 ± 0.06	0.34 ± 0.04	13.03	< .001[a]
Window 4 (600–900 ms)	0.40 ± 0.06	0.37 ± 0.05	2.58	.115
Window 5 (900–1200 ms)	0.43 ± 0.06	0.44 ± 0.04	0.50	.482
Global Efficiency NOGO				
Baseline	0.47 ± 0.05	0.47 ± 0.04	0.04	.839
Static window (0–1200 ms)	0.46 ± 0.03	0.43 ± 0.06	4.95	.03
Window 2 (0–300 ms)	0.46 ± 0.05	0.40 ± 0.04	27.18	< .001[a]
Window 3 (300–600 ms)	0.40 ± 0.05	0.32 ± 0.04	41.68	< .001[a]
Window 4 (600–900 ms)	0.43 ± 0.06	0.42 ± 0.05	0.39	.537
Window 5 (900–1200 ms)	0.47 ± 0.05	0.47 ± 0.05	0.21	.648
Clustering Coefficient GO				
Baseline	0.20 ± 0.04	0.20 ± 0.02	0.14	.698
Static window (0–1200 ms)	0.21 ± 0.03	0.24 ± 0.03	11.79	.001[a]
Window 2 (0–300 ms)	0.24 ± 0.03	0.28 ± 0.02	24.10	< .001[a]
Window 3 (300–600 ms)	0.25 ± 0.03	0.28 ± 0.01	20.13	< .001[a]
Window 4 (600–900 ms)	0.24 ± 0.03	0.26 ± 0.02	9.59	.003[a]
Window 5 (900–1200 ms)	0.22 ± 0.04	0.22 ± 0.03	0.05	.822
Clustering Coefficient NOGO				
Baseline	0.20 ± 0.03	0.20 ± 0.03	0.14	.713
Static window (0–1200 ms)	0.18 ± 0.02	0.21 ± 0.02	26.16	< .001[a]
Window 2 (0–300 ms)	0.21 ± 0.03	0.24 ± 0.02	20.17	< .001[a]
Window 3 (300–600 ms)	0.23 ± 0.03	0.27 ± 0.01	39.45	< .001[a]
Window 4 (600–900 ms)	0.21 ± 0.04	0.23 ± 0.02	1.89	.176
Window 5 (900–1200 ms)	0.20 ± 0.03	0.20 ± 0.03	1.66	.204

Data are mean ± SD.
[a]$p < .01$.

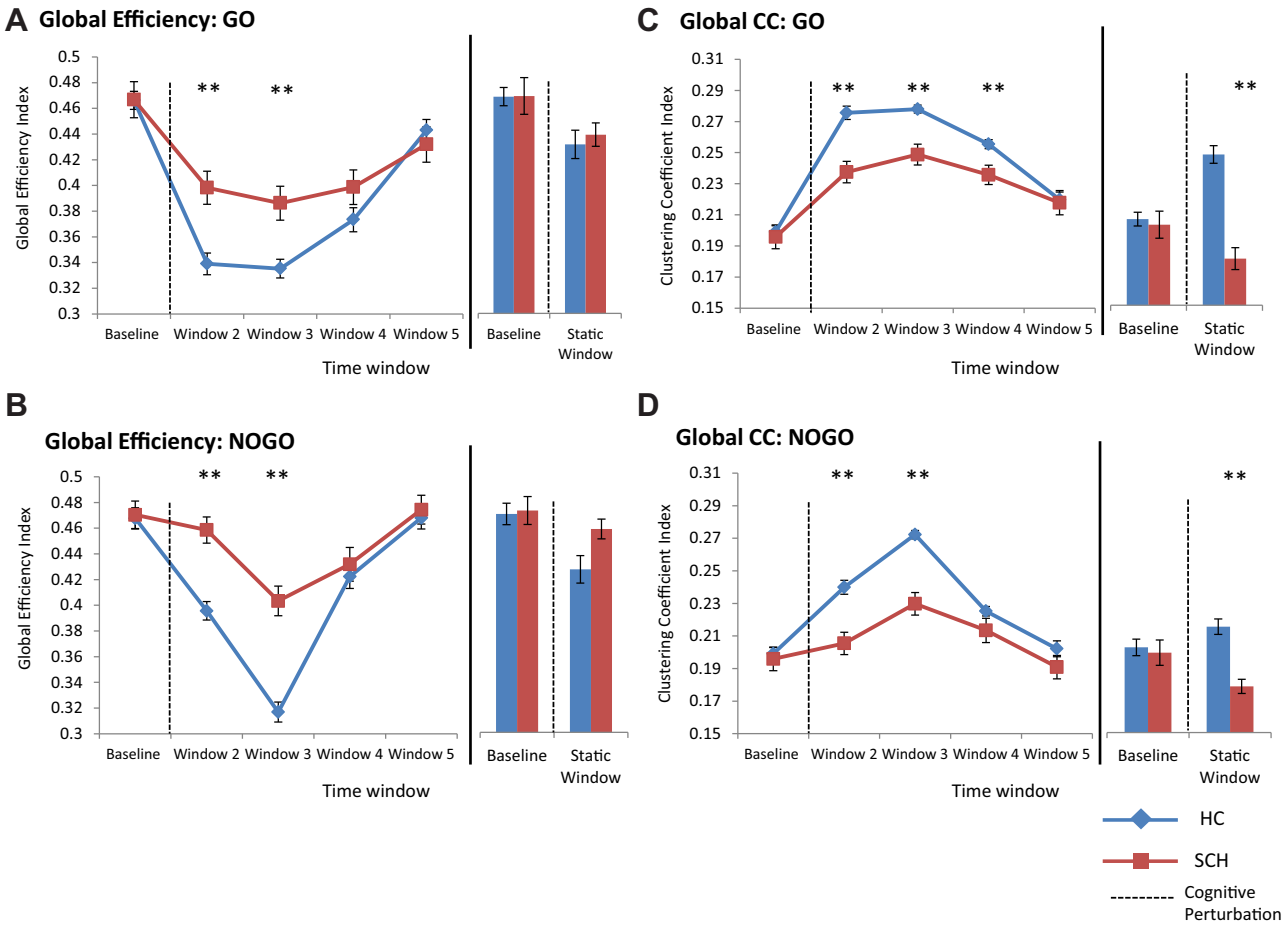

Figure 1. Global network connectivity. Shown are group means and standard errors across the global network metrics for patients with schizophrenia (SCH) and healthy control (HC) subjects. Presented are the dynamic network (left) and static network (right) responses to the cognitive perturbation (Sustained Attention to Response Task) according to the following global metrics: **(A)** global efficiency: GO; **(B)** global efficiency: NOGO; **(C)** global clustering coefficient (CC): GO; and **(D)** global CC: NOGO. These network metrics are monitored across baseline and dynamic and static time windows: baseline (−350 to −50 ms), window 2 (0 to 300 ms), window 3 (300 to 600 ms), window 4 (600 to 900 ms), window 5 (900 to 1200 ms), and the static window (0 to 1200 ms). $^{**}p < .01$.

frontal, temporal, sensory-motor, and parietal regions at window 2 and showed reduced CC of the frontal, sensory-motor, parietal, and occipital regions at window 3. No significant differences between groups were found at windows 4 and 5 (see Figure 2 and Table 3).

Regional Measures: Strength. In the GO condition, at baseline the SCH group demonstrated increased strength in the sensory-motor region. In the static network, the SCH group presented with reduced strength in the frontal regions. In the dynamic network, the SCH group showed decreased strength in the occipital region at window 2, reduced strength in the frontal, sensory-motor, and parietal regions, and increased strength in the occipital region at window 3, and reduced strength in the frontal regions at window 4. By window 5, the SCH group showed increased strength of the sensory-motor region (similar to baseline).

In the NOGO condition, at baseline there were no significant differences between groups. In the static network, the SCH group presented with reduced strength in the frontal, parietal, and occipital regions. In the dynamic network, the SCH group exhibited reduced strength at window 3 in the frontal, sensory-motor, parietal, and occipital regions (mid) while presenting with increased strength in the occipital region (left). There were no significant differences between groups at windows 2, 4, and 5 (see Figure 2 and Table 4).

Clinical Relevance of Network Measures

In terms of clinical measures, strength of the frontal region at window 4 positively related to Scale for the Assessment of Negative Symptoms total ($r = .590$, $n = 21$, $p = .005$), whereas strength of the sensory-motor region at window 5 was negatively associated with Scale for the Assessment of Positive Symptoms total ($r = -.620$, $n = 21$, $p = .003$). In the static network, strength of the parietal region positively correlated with Scale for the Assessment of Negative Symptoms total ($r = .567$, $n = 21$, $p = .007$). With regard to neurological measures, strength of the sensory-motor regions at windows 3 and 4 correlated positively with Neurological Evaluation Scale symptoms ($r = .576$, $n = 21$, $p = .006$, and $r = .623$, $n = 21$, $p = .003$,

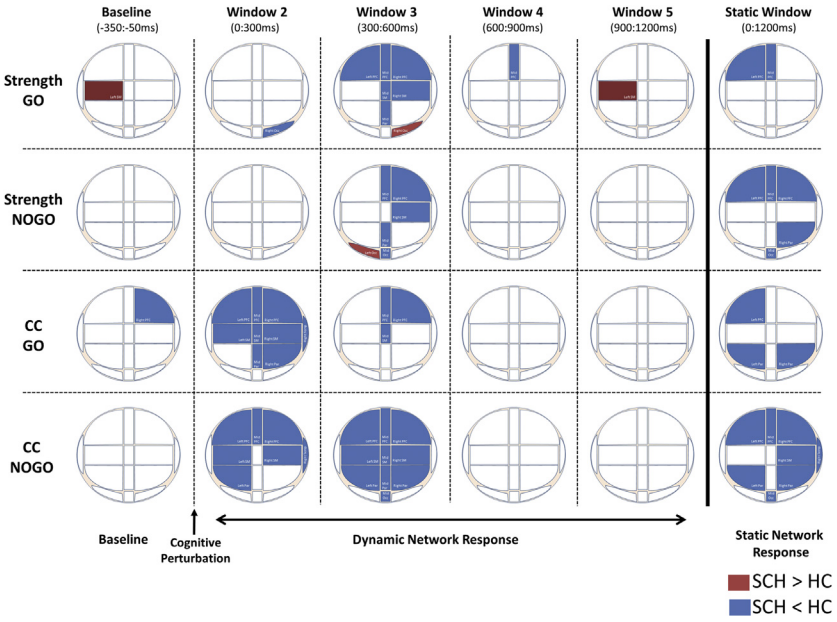

Figure 2. Regional network connectivity. Shown are significant differences in regional network metrics (local strength and clustering coefficient [CC]) for patients with schizophrenia (SCH) and healthy control (HC) subjects. This figure demonstrates how the dynamic network (left) and static network (right) patterns of response to the cognitive perturbation (Sustained Attention to Response Task) differ significantly between groups (when $p < .01$). Red regions reflect areas in which local network metrics (strength and CC) of SCH patients are significantly higher than in the HC group, and blue regions represent areas in which the local network metrics of SCH patients are significantly lower than in the HC group. The division of brain regions is further described in Supplemental Figure S6.

respectively). For cognitive symptoms, we found that CC of the right sensory-motor and parietal regions at baseline positively correlated with increased attentional symptoms ($r = .643$, $n = 21$, $p = .002$, and $r = .602$, $n = 21$, $p = .004$, respectively). No further significant correlations were observed.

ROC curve analysis also demonstrated that approximately 95% of test variables (network metrics), which differed significantly between the groups, were capable of discriminating between the SCH group and the HC group (see the Supplement).

DISCUSSION

The current study characterized anomalies in dynamic network connectivity underlying specific cognitive features of SCH. The dynamic approach enabled us to reveal a broad range of time-sensitive network connectivity alterations in the SCH group. For the SCH group, the cognitive stimuli elicited widespread decreased segregation and increased global integration while also activating peripheral hub regions in place of task-relevant regions. Network differences were temporally sensitive, and the network configuration returned to comparable levels with HC participants at 900 ms following the cognitive perturbation (similar to baseline). Therefore, our study emphasizes the importance of characterizing the dynamic nature of these network anomalies when studying cognition in SCH.

Cognition and Dynamic Networks in SCH

As expected, the SART identified impaired inhibition and sustained attention in the SCH group (32,34,45,46). In the current study, however, stimuli from the SART were applied as a cognitive method to perturb (induce a transient change within) the network organization while EEG quantified the functional dynamics of the network response. We found that SART stimuli were capable of successfully perturbing the brain network and eliciting a measurable dynamic change in the network. These effects resemble the transient changes in SCH networks elicited by transcranial magnetic stimulation perturbations in our previous study (47). In the current study, patients with SCH showed altered patterns of network organization in response to the cognitive stimuli (perturbations) across both global and regional connectivity measures.

Global Connectivity

Static network analysis revealed that the SCH group exhibited reduced global segregation (CC) in response to the cognitive stimuli, whereas no difference was observed in global integration (GE). Reduced CC is consistently observed in the literature (22,26,27,29), whereas findings regarding GE are often mixed (22,27,29). In the past, characterization of these global measures relied on static representations of the connectivity patterns. However, given that cognition relies on dynamic coordination of widely distributed brain regions, it is critical to examine the dynamic nature of these networks to advance our understanding of network connectivity underlying cognitive features of SCH.

We examined this concept by applying dynamic network analysis to characterize how network connectivity patterns evolve over time. Using this dynamic network approach, our study uncovered that the SCH group presented with significantly reduced global segregation (CC) (27,48) and increased integration (GE) (26,48) relative to the HC group. These network differences were pronounced within the first 900 ms following the cognitive perturbation before returning to comparable levels with HC participants. Importantly, SCH patients exhibited a similar trajectory of global network response to that of HC participants, but this response occurred at significantly lower amplitude. Optimal network structure underlying adequate cognitive function relies on the delicate balance between segregation and integration of specialized brain regions (22,49,50). Therefore, an intriguing possibility is that

Table 3. Regional Connectivity Measures: Local Clustering Coefficient Indices That Were Significantly Different Across the GO and NOGO Conditions in Patients With Schizophrenia and Healthy Control Participants

	Patients With Schizophrenia (n = 21)	Healthy Control Participants (n = 28)	F Value, df = (1,47)	p Value
Local Clustering GO				
Baseline				
Right prefrontal cortex	0.16 ± 0.04	0.19 ± 0.03	8.18	.006[a]
Static window (0–1200 ms)				
Left prefrontal cortex	0.20 ± 0.03	0.23 ± 0.03	11.10	.002[a]
Left parietal	0.21 ± 0.03	0.24 ± 0.03	11.76	.001[a]
Right parietal	0.21 ± 0.03	0.24 ± 0.04	8.05	.007[a]
Window 2 (0–300 ms)				
Left prefrontal cortex	0.21 ± 0.04	0.25 ± 0.05	8.26	.006[a]
Right prefrontal cortex	0.22 ± 0.05	0.26 ± 0.05	11.26	.002[a]
Mid prefrontal cortex	0.24 ± 0.06	0.29 ± 0.06	8.05	.007[a]
Right temporal	0.23 ± 0.05	0.29 ± 0.04	15.56	< .001[a]
Left sensory-motor	0.24 ± 0.04	0.29 ± 0.04	17.66	< .001[a]
Right sensory-motor	0.24 ± 0.04	0.30 ± 0.04	23.73	< .001[a]
Mid sensory-motor	0.24 ± 0.04	0.28 ± 0.05	12.03	.001[a]
Right parietal	0.26 ± 0.04	0.29 ± 0.04	8.10	.007[a]
Mid parietal	0.24 ± 0.03	0.28 ± 0.04	15.02	< .001[a]
Window 3 (300–600 ms)				
Right prefrontal cortex	0.21 ± 0.05	0.27 ± 0.04	20.32	< .001[a]
Mid prefrontal cortex	0.27 ± 0.08	0.33 ± 0.04	12.41	< .001[a]
Mid sensory-motor	0.28 ± 0.06	0.32 ± 0.05	10.47	.002[a]
Local Clustering NOGO				
Static window (0–1200 ms)				
Left prefrontal cortex	0.18 ± 0.03	0.22 ± 0.03	22.23	< .001[a]
Right prefrontal cortex	0.17 ± 0.03	0.21 ± 0.04	18.86	< .001[a]
Mid prefrontal cortex	0.18 ± 0.04	0.23 ± 0.05	14.86	< .001[a]
Right temporal	0.18 ± 0.04	0.21 ± 0.04	7.82	.007[a]
Right sensory-motor	0.17 ± 0.03	0.21 ± 0.04	14.98	< .001[a]
Left parietal	0.19 ± 0.03	0.22 ± 0.03	15.99	< .001[a]
Right parietal	0.18 ± 0.03	0.22 ± 0.03	18.68	< .001[a]
Mid occipital	0.19 ± 0.05	0.24 ± 0.06	8.01	.007[a]
Window 2 (0–300 ms)				
Left prefrontal cortex	0.18 ± 0.04	0.22 ± 0.04	17.39	< .001[a]
Right prefrontal cortex	0.18 ± 0.04	0.22 ± 0.04	13.59	< .001[a]
Mid prefrontal cortex	0.21 ± 0.04	0.27 ± 0.03	26.14	< .001[a]
Right temporal	0.19 ± 0.04	0.22 ± 0.05	7.70	.007[a]
Left sensory-motor	0.22 ± 0.04	0.26 ± 0.03	11.72	.001[a]
Right sensory-motor	0.22 ± 0.05	0.25 ± 0.03	8.00	.006[a]
Left parietal	0.23 ± 0.04	0.26 ± 0.03	11.49	.001[a]
Window 3 (300–600 ms)				
Left prefrontal cortex	0.22 ± 0.05	0.26 ± 0.04	11.39	.001[a]
Right prefrontal cortex	0.20 ± 0.04	0.26 ± 0.05	20.93	< .001[a]
Mid prefrontal cortex	0.25 ± 0.07	0.31 ± 0.05	13.09	< .001[a]
Left sensory-motor	0.25 ± 0.05	0.30 ± 0.06	8.98	.004[a]
Right sensory-motor	0.26 ± 0.06	0.32 ± 0.05	15.71	< .001[a]
Mid sensory-motor	0.26 ± 0.04	0.33 ± 0.05	35.91	< .001[a]
Left parietal	0.25 ± 0.04	0.29 ± 0.04	17.06	< .001[a]
Right parietal	0.24 ± 0.05	0.29 ± 0.04	14.55	< .001[a]
Mid parietal	0.26 ± 0.04	0.33 ± 0.06	25.91	< .001[a]
Mid occipital	0.24 ± 0.06	0.34 ± 0.06	30.54	< .001[a]

Data are mean ± SD.
[a]$p < .01$.

Table 4. Regional Connectivity Measures: Local Strength Indices That Were Significantly Different Across the GO and NOGO Conditions in Patients With Schizophrenia and Healthy Control Participants

	Patients With Schizophrenia (n = 21)	Healthy Control Participants (n = 28)	F Value, df = (1,47)	p Value
Local Strength GO				
Baseline				
Left sensory-motor	73.97 ± 16.39	61.42 ± 12.99	8.95	.004[a]
Static window (0–1200 ms)				
Left prefrontal cortex	41.96 ± 11.02	52.22 ± 11.35	10.07	.003[a]
Mid prefrontal cortex	56.63 ± 18.01	81.75 ± 24.08	16.06	< .00[a]
Window 2 (0–300 ms)				
Right occipital	63.29 ± 22.09	88.89 ± 23.21	15.20	< .00[a]
Window 3 (300–600 ms)				
Left prefrontal cortex	42.80 ± 15.22	63.61 ± 20.82	14.95	< .001[a]
Right prefrontal cortex	45.08 ± 17.20	65.74 ± 19.69	14.69	< .001[a]
Mid prefrontal cortex	75.19 ± 25.23	103.53 ± 28.14	13.28	< .001[a]
Right sensory-motor	80.20 ± 19.08	103.10 ± 19.36	17.00	< .001[a]
Mid sensory-motor	90.26 ± 28.92	115.30 ± 26.09	10.07	.004[a]
Mid parietal	88.93 ± 23.79	115.75 ± 34.77	9.23	.004[a]
Right occipital	77.95 ± 20.02	58.43 ± 26.47	7.57	.008[a]
Window 4 (600–900 ms)				
Mid prefrontal cortex	67.83 ± 31.08	91.39 ± 29.26	7.38	.009[a]
Window 5 (900–1200 ms)				
Left sensory-motor	80.20 ± 12.45	67.55 ± 17.36	8.03	.006[a]
Local Strength NOGO				
Static window (0–1200 ms)				
Left prefrontal cortex	41.22 ± 10.48	54.16 ± 10.75	17.76	< .001[a]
Right prefrontal cortex	39.47 ± 12.19	55.49 ± 14.36	16.94	< .001[a]
Mid prefrontal cortex	62.94 ± 17.63	87.20 ± 22.42	16.77	< .001[a]
Right parietal	48.29 ± 10.07	57.23 ± 8.56	11.24	.002[a]
Mid occipital	59.81 ± 19.41	77.96 ± 22.23	8.90	.005[a]
Window 3 (300–600 ms)				
Right prefrontal cortex	42.29 ± 10.69	69.99 ± 16.87	43.45	< .001[a]
Mid prefrontal cortex	69.21 ± 28.76	123.68 ± 16.58	69.85	< .001[a]
Right sensory-motor	77.73 ± 15.23	91.37 ± 16.64	8.66	.005[a]
Mid parietal	84.90 ± 25.06	108.26 ± 28.24	9.03	.004[a]
Mid occipital	71.32 ± 32.98	99.61 ± 33.62	8.63	.005[a]
Left occipital	72.53 ± 22.50	52.29 ± 20.06	11.01	.002[a]

Data are mean ± SD.
[a]$p < .01$.

patients with SCH compensate for a less globally segregated (reduced CC) network by recruiting a larger number of peripheral brain regions concurrently (shorter path lengths) to achieve successful performance on the SART.

Moreover, the reduced trajectory of network response in the SCH group may reflect impaired network flexibility in response to a cognitive perturbation (12,13,18). Previous studies demonstrated that increased flexibility of network response was predictive of increased learning (12) and adaptability to cognitive demands (13). If we apply this notion to our study, then the increased range of segregation and integration in the HC network may allow HC participants to more flexibly meet cognitive demands by delicately balancing these global measures. The SCH group, on the other hand, presented with a reduced range of segregation and integration, and it is possible that an altered balance between these global measures may represent a less flexible state.

Regional Connectivity

In terms of regional connectivity, static network analysis revealed that the SCH group recruited a less frontal and centralized network (strength) and demonstrated evidence of widespread reduced segregation (local CC) compared with the HC group. Evidence of the emergence of nonfrontal hubs in SCH have been demonstrated across static functional magnetic resonance imaging (51–55), diffusion tensor imaging studies (56–58), and transcranial magnetic stimulation studies (47). Only a small number of EEG studies have explored regional connectivity alterations in SCH (22,29) given that the focus is usually on global measures of connectivity.

When we applied dynamic network analysis, we found that dynamic patterns of network organization correlated with clinical symptoms of the SCH group. Moreover, the dynamic network approach increased the sensitivity of our analysis and led to the identification of a broader number of regional differences in SCH. SCH presented with reduced strength and decreased local CC (segregation around specific nodes) around the frontal, parietal, and sensory-motor areas while showing increased strength around the occipital lobes (a peripheral hub). These network differences were prominent within the first 900 ms following the cognitive perturbation before returning to comparable levels as in the HC group. Patients with SCH also demonstrated significantly increased sensory-motor strength at baseline (and at 900–1200 ms), and these increases in strength were capable of discriminating between patients with SCH and HC participants (ROC analysis). Moreover, increased CC of the sensory-motor and parietal regions at baseline was related to increased symptoms of attentional deficits in SCH. While these findings are not conclusive yet, when combined they provide initial support for the use of regional network measures as potential biomarkers of SCH.

Successful performance on the SART relies on the integrity of frontal and parietal regions for executive control (2,35,59), whereas the sensory-motor region has a pivotal role in the functional integration between these cognitive networks and the execution of voluntary movements (60). These brain regions are considered highly interconnected and functionally integrated with many regions of the brain. Therefore, it is logical that these regions relate to clinical (frontal and parietal regions) and neurological (sensory-motor) symptoms of SCH as well as being predictive of the disease state. For the HC group, successful task performance relies on increased integration of these task-relevant regions and decreased integration of the peripheral regions (18). Therefore, our opposite finding of reduced integration of these major task-relevant regions and the recruitment of peripheral regions by the SCH group (even when successfully completing the task) provide strong empirical support for the presence of altered dynamic network organization underlying day-to-day features of cognition.

Limitations

Although these findings provide compelling evidence of network anomalies underlying cognition in the SCH group, several methodological issues should be considered. First, given that all SCH participants were undergoing antipsychotic drug treatment, we are unable to separate the potential effects of antipsychotic medications from our results. We did examine the effect of medication type (atypical vs. typical antipsychotic medication) on network metrics and observed no significant changes in the current findings. Therefore, our results should be considered as representative of an inpatient and medicated SCH population. Second, while HC participants and SCH patients were matched for age, gender, and handedness, they differed in years of education. To address this limitation, we examined the analysis of variance across all variables with years of education as a covariate and found that all reported significant differences remained relevant. Third, across the network studies, there are a vast number of methods for network construction, thresholding, and reference choice when applying graph theory to neuroimaging data. We applied a standard network construction technique (Pearson correlation) that is based on the cross-correlation between EEG signals (5). Notably, we do not directly measure anatomical connectivity; rather, network connectivity is inferred from correlations between EEG traces. Fourth, further studies are required to discern whether these network effects are specific to SCH or represent a more general indicator of cognitive impairment. Given the multifaceted nature of cognition, it would be worthwhile to examine whether these cognitive results are specific to the SART or vary according to the cognitive construct being examined. Fifth, the study sample was limited in size, and multiple comparisons were conducted for the regional network and correlation values. To address this, a conservative alpha value of significance ($p < .01$) was implemented, and the utility of the test measures was examined via the ROC curve analysis (to evaluate their ability to discriminate between SCH patients and HC participants). Therefore, results from the current study should be considered as indicative rather than conclusive, and further studies are required to fully validate our findings.

Conclusions

Our study provided quantitative measures of the dynamic network anomalies underlying specific cognitive features of SCH. The SCH group demonstrated temporally sensitive network alterations across both the global and regional connectivity measures in response to the cognitive stimuli. More specifically, SCH patients exhibited decreased CC (segregation), increased efficiency (integration), and reduced integration of major task-relevant regions (and increased recruitment of peripheral hub regions). These network aberrations may indicate the presence of altered integration and segregation processes underlying specific cognitive features of SCH. Therefore, our study highlights the importance of examining dynamic patterns of network connectivity in better understanding cognitive features of SCH. It is hoped that identification of the network anomalies underlying key symptoms of SCH will improve our understanding of SCH and lead to the development of network biomarkers to improve current diagnosis and treatment models.

ACKNOWLEDGMENTS AND DISCLOSURES

JN-F is a recipient of the Senior Postdoctoral Fellowship at the Weizmann Institute, the Curwen-Lowy Postdoctoral Fellowship, and the Clore Postdoctoral Fellowship that supported the development of this study. EM is supported by the Minerva Foundation (Germany) and by the Israel Science Foundation. The study was supported by NL-B's Israel Science Foundation grant (No. 1169/11) and by the National Institute of Psychobiology in Israel.

We thank Dana Koresh and Shir Yerushalmi for their assistance with data acquisition and to Dana Tel-Zur for her contribution in preprocessing the EEG data.

The authors report no biomedical financial interests or potential conflicts of interest.

ARTICLE INFORMATION

From the Department of Physics of Complex Systems (JN-F, MR, DF, EM), Weizmann Institute of Science, Rehovot; Sagol Center for Brain and Mind (JN-F, DF, NL-B), Baruch Ivcher School of Psychology, Interdisciplinary Center (IDC), Herzliya; Institute for Psychiatric Studies (AG, AP), Sha'ar Menashe Mental Health Center, Sha'ar Menashe; and Ruth and Bruce

Rappaport Faculty of Medicine (AG, AP), Technion, Israel Institute of Technology, Haifa, Israel.

EM and NL-B contributed equally to this work.

Address correspondence to Jodie Naim-Feil, Ph.D., Department of Physics of Complex Systems, Weizmann Institute of Science, Herzl St. 234, Rehovot 7610001, Israel; E-mail: jodie@naimfeil.org.

Received Dec 25, 2016; revised Mar 8, 2017; accepted Mar 11, 2017.

Supplementary material cited in this article is available online at http://dx.doi.org/10.1016/j.bpsc.2017.03.017.

REFERENCES

1. Keefe RSE, Harvey PD (2012): Novel antischizophrenia treatments. In: Geyer MA, Gross G, editors. Handbook of Experimental Pharmacology, vol. 213. New York: Springer, pp. 11–38.
2. Garavan H (2002): Dissociable executive functions in the dynamic control of behavior: Inhibition, error detection, and correction. NeuroImage 17:1820–1829.
3. Shenton ME, Dickey CC, Frumin M, McCarley RW (2001): A review of MRI findings in schizophrenia. Schizophr Res 49:1–52.
4. Tan HY, Callicott JH, Weinberger DR (2007): Dysfunctional and compensatory prefrontal cortical systems, genes and the pathogenesis of schizophrenia. Cereb Cortex 17:171–181.
5. Stam CJ, Reijneveld JC (2007): Graph theoretical analysis of complex networks in the brain. Nonlinear Biomed Phys 1:3.
6. van Straaten ECW, Stam CJ (2013): Structure out of chaos: Functional brain network analysis with EEG, MEG, and functional MRI. Eur Neuropsychopharmacol 23:7–18.
7. Bullmore ET, Sporns O (2009): Complex brain networks: Graph theoretical analysis of structural and functional systems. Nat Rev Neurosci 10:186–198.
8. Bleuler E (1911): Dementia Praecox or the Goup of Schizophrenias (English ed., 1950). New York: International University Press.
9. Friston KJ, Frith CD (1995): Schizophrenia: A disconnection syndrome? Clin Neurosci 3:89–97.
10. Fornito A, Zalesky A, Pantelis C, Bullmore ET (2012): Schizophrenia, neuroimaging, and connectomics. NeuroImage 62:2296–2314.
11. Telesford QK, Lynall M-E, Vettel J, Miller MB, Grafton ST, Bassett DS (2016): Detection of functional brain network reconfiguration during task-driven cognitive states. NeuroImage 142:198–210.
12. Bassett DS, Wymbs NF, Porter MA, Mucha PJ, Carlson JM, Grafton ST (2010): Dynamic reconfiguration of human brain networks during learning. Proc Natl Acad Sci U S A 108:7641–7646.
13. Braun U, Schäfer A, Walter H, Erk S, Romanczuk-Seiferth N, Haddad L, *et al.* (2015): Dynamic reconfiguration of frontal brain networks during executive cognition in humans. Proc Natl Acad Sci U S A 112:11678–11683.
14. Dasari NM, Nandagopal ND, Ramasamy V, Cocks B, Thomas BH, Dahal N, Gaertner P (2015): Moment to moment variability in functional brain networks during cognitive activity in EEG data. J Integr Neurosci 14:383–402.
15. McIntosh AR (2000): Towards a network theory of cognition. Neural Netw 13:861–870.
16. Medaglia JD, Lynall M-E, Bassett DS (2015): Cognitive network neuroscience. J Cogn Neurosci 27:1471–1491.
17. Davison EN, Schlesinger KJ, Bassett DS, Lynall ME, Miller MB, Grafton ST, Carlson JM (2015): Brain network adaptability across task states. PLoS Comput Biol 11:e1004029.
18. Ekman M, Derrfuss J, Tittgemeyer M, Fiebach CJ (2012): Predicting errors from reconfiguration patterns in human brain networks. Proc Natl Acad Sci U S A 109:16714–16719.
19. Kitzbichler MG, Henson RNA, Smith ML, Nathan PJ, Bullmore ET (2011): Cognitive effort drives workspace configuration of human brain functional networks. J Neurosci 31:8259–8270.
20. Bola M, Sabel BA (2015): Dynamic reorganization of brain functional networks during cognition. NeuroImage 114:398–413.
21. Wei L, Li Y, Yang X, Xue Q, Wang Y (2015): Altered characteristic of brain networks in mild cognitive impairment during a selective attention task: An EEG study. Int J Psychophysiol 98:8–16.
22. Rubinov M, Knock SA, Stam CJ, Micheloyannis S, Harris AWF, Williams LM, Breakspear M (2009): Small-world properties of nonlinear brain activity in schizophrenia. Hum Brain Mapp 30:403–416.
23. Breakspear M, Terry J, Friston K, Harris AW, Williams L, Brown K, *et al.* (2003): A disturbance of nonlinear interdependence in scalp EEG of subjects with first episode schizophrenia. NeuroImage 20:466–478.
24. Sheffield JM, Repovs G, Harms MP, Carter CS, Gold JM, MacDonald AW, *et al.* (2015): Fronto-parietal and cingulo-opercular network integrity and cognition in health and schizophrenia. Neuropsychologia 73:82–93.
25. De Vico Fallani F, Maglione A, Babiloni F, Mattia D, Astolfi L, Vecchiato G, *et al.* (2010): Cortical network analysis in patients affected by schizophrenia. Brain Topogr 23:214–220.
26. Pachou E, Vourkas M, Simos P, Smit D, Stam CJ, Tsirka V, Micheloyannis S (2008): Working memory in schizophrenia: An EEG study using power spectrum and coherence analysis to estimate cortical activation and network behavior. Brain Topogr 21:128–137.
27. Micheloyannis S, Pachou E, Stam CJ, Breakspear M, Bitsios P, Vourkas M, *et al.* (2006): Small-world networks and disturbed functional connectivity in schizophrenia. Schizophr Res 87:60–66.
28. Jhung K, Cho S-H, Jang J-H, Park JY, Shin D, Kim KR, *et al.* (2013): Small-world networks in individuals at ultra-high risk for psychosis and first-episode schizophrenia during a working memory task. Neurosci Lett 535:35–39.
29. Shim M, Kim D-W, Lee S-H, Im C-H (2014): Disruptions in small-world cortical functional connectivity network during an auditory oddball paradigm task in patients with schizophrenia. Schizophr Res 156:197–203.
30. Robertson IH, Manly T, Andrade J, Baddeley BT, Yiend J (1997): "Oops!": Performance correlates of everyday attentional failures in traumatic brain injured and normal subjects. Neuropsychologia 35:747–758.
31. Helton WS, Kern RP, Walker DR (2009): Conscious thought and the sustained attention to response task. Conscious Cogn 18:600–607.
32. Chan RCK, Wang Y, Cheung EFC, Cui J, Deng Y, Yuan Y, *et al.* (2009): Sustained attention deficit along the psychosis proneness continuum: A study on the Sustained Attention to Response Task (SART). Cogn Behav Neurol 22:180–185.
33. Chan RCK, Chen EYH, Cheung EFC, Chen RYL, Cheung HK (2004): A study of sensitivity of the sustained attention to response task in patients with schizophrenia. Clin Neuropsychol 18:114–121.
34. O'Gráda C, Barry S, McGlade N, Behan C, Haq F, Hayden J, *et al.* (2009): Does the ability to sustain attention underlie symptom severity in schizophrenia? Schizophr Res 107:319–323.
35. Dockree PM, Kelly SP, Robertson IH, Reilly RB, Foxe JJ (2005): Neurophysiological markers of alert responding during goal-directed behavior: A high-density electrical mapping study. NeuroImage 27:587–601.
36. Erika-Florence M, Leech R, Hampshire A (2014): A functional network perspective on response inhibition and attentional control. Nat Commun 5:4073.
37. American Psychiatric Association (2000): Diagnostic and Statistical Manual of Mental Disorders, 4th ed. Washington, DC: American Psychiatric Press.
38. Andreasen NC (1984): The Scale for the Assessment of Positive Symptoms (SAPS). Iowa City: University of Iowa College of Medicine.
39. Andreasen NC (1989): The Scale for the Assessment of Negative Symptoms (SANS): Conceptual and Theoretical Foundations. Br J Psychiatry Suppl:49–58.
40. Buchanan RW, Heinrichs DW (1989): The Neurological Evaluation Scale (NES): A structured instrument for the assessment of neurological signs in schizophrenia. Psychiatry Res 27:335–350.
41. Delorme A, Makeig S (2004): EEGLAB: An open source toolbox for analysis of single-trial EEG dynamics including independent component analysis. J Neurosci Methods 134:9–21.
42. Rubinov M, Sporns O (2010): Complex network measures of brain connectivity: Uses and interpretations. NeuroImage 52:1059–1069.

43. Varela F, Lachaux JP, Rodriguez E, Martinerie J (2001): The brainweb: Phase synchronization and large-scale integration. Nat Rev Neurosci 2:229–239.
44. Eckmann J-P, Moses E (2002): Curvature of co-links uncovers hidden thematic layers in the World Wide Web. Proc Natl Acad Sci U S A 99:5825–5829.
45. Chan RCK, Chen EYH (2004): Executive dysfunctions and neurological manifestations in schizophrenia. Hong Kong Psychiatry 14:2–6.
46. Seok J-H, Park H-J, Lee J-D, Kim H-S, Chun J-W, Son SJ, *et al.* (2012): Regional cerebral blood flow changes and performance deficit during a sustained attention task in schizophrenia: O-water positron emission tomography. Psychiatry Clin Neurosci 66:564–572.
47. Arzouan Y, Moses E, Peled A, Levit-Binnun N (2014): Impaired network stability in schizophrenia revealed by TMS perturbations. Schizophr Res 152:322–324.
48. He H, Sui J, Yu Q, Turner JA, Ho B-C, Sponheim SR, *et al.* (2012): Altered small-world brain networks in schizophrenia patients during working memory performance. PLoS One 7:e38195.
49. Tononi G, Sporns O, Edelman GM (1994): A measure for brain complexity: Relating functional segregation and integration in the nervous system. Proc Natl Acad Sci U S A 91:5033–5037.
50. Deco G, Tononi G, Boly M, Kringelbach ML (2015): Rethinking segregation and integration: Contributions of whole-brain modelling. Nat Rev Neurosci 16:430–439.
51. Fornito A, Yoon J, Zalesky A, Bullmore ET, Carter CS (2011): General and specific functional connectivity disturbances in first-episode schizophrenia during cognitive control performance. Biol Psychiatry 70:64–72.
52. Alexander-Bloch AF, Gogtay N, Meunier D, Birn R, Clasen L, Lalonde F, *et al.* (2010): Disrupted modularity and local connectivity of brain functional networks in childhood-onset schizophrenia. Front Syst Neurosci 4:147.
53. Lynall M-E, Bassett DS, Kerwin R, McKenna PJ, Kitzbichler M, Muller U, Bullmore E (2010): Functional connectivity and brain networks in schizophrenia. J Neurosci 30:9477–9487.
54. Cole MW, Anticevic A, Repovs G, Barch D (2011): Variable global dysconnectivity and individual differences in schizophrenia. Biol Psychiatry 70:43–50.
55. Bassett DS, Bullmore E, Verchinski BA, Mattay VS, Weinberger DR, Meyer-Lindenberg A (2008): Hierarchical organization of human cortical networks in health and schizophrenia. J Neurosci 28: 9239–9248.
56. Wang Q, Su T-P, Zhou Y, Chou K-H, Chen I-Y, Jiang T, Lin C-P (2012): Anatomical insights into disrupted small-world networks in schizophrenia. NeuroImage 59:1085–1093.
57. Sun Y, Chen Y, Lee R, Bezerianos A, Collinson SL, Sim K (2016): Disruption of brain anatomical networks in schizophrenia: A longitudinal, diffusion tensor imaging based study. Schizophr Res 171: 149–157.
58. van den Heuvel MP, Mandl RC, Stam CJ, Kahn RS, Hulshoff Pol HE (2010): Aberrant frontal and temporal complex network structure in schizophrenia: A graph theoretical analysis. J Neurosci 30: 15915–15926.
59. Naim-Feil J, Bradshaw JL, Sheppard DM, Rosenberg O, Levkovitz Y, Dannon P, *et al.* (2016): Neuromodulation of attentional control in major depression: A pilot deep TMS study [published online ahead of print Dec 28]. Neural Plast.
60. Simmons DJ, Pekar JJ, Mostofsky SH (2008): Meta-analysis of Go/No-go tasks demonstrating that fMRI activation associated with response inhibition is task-dependent. Neuropsychologia 46:224–232.